Heliyon 10 (2024) e40588

Contents lists available at ScienceDirect

Heliyon

journal homepage: www.cell.com/heliyon

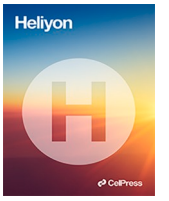

Review article

Radiomics predicting immunohistochemical markers in primary hepatic carcinoma: Current status and challenges

Yunqing Yin [a,1], Wei Zhang [b,1], Yanhui Chen [c], Yanfang Zhang [b,*], Xinying Shen [b,**]

[a] The Second Clinical Medical College, Jinan University, China
[b] Department of Intervention, Shenzhen People's Hospital, Shenzhen, 518020, Guangdong, China
[c] Department of Intervention, Shenzhen Bao'an People's Hospital, Shenzhen, 518100, Guangdong, China

ARTICLE INFO

Keywords:
Radiomics
Primary hepatic carcinoma
Immunohistochemical markers
Magnetic resonance imaging
Ultrasound
Computed tomography

ABSTRACT

Primary hepatic carcinoma, comprising hepatocellular carcinoma (HCC), intrahepatic cholangiocarcinoma (ICC), and combined hepatocellular cholangiocarcinoma (cHCC-CCA), ranks among the most common malignancies worldwide. The heterogeneity of tumors is a primary factor impeding the efficacy of treatments for primary hepatic carcinoma. Immunohistochemical markers may play a potential role in characterizing this heterogeneity, providing significant guidance for prognostic analysis and the development of personalized treatment plans for the patients with primary hepatic carcinoma. Currently, primary hepatic carcinoma immunohistochemical analysis primarily relies on invasive techniques such as surgical pathology and tissue biopsy. Consequently, the non-invasive preoperative acquisition of primary hepatic carcinoma immunohistochemistry has emerged as a focal point of research. As an emerging non-invasive diagnostic technique, radiomics possesses the potential to extensively characterize tumor heterogeneity. It can predict immunohistochemical markers associated with hepatocellular carcinoma preoperatively, demonstrating significant auxiliary utility in clinical guidance. This article summarizes the progress in using radiomics to predict immunohistochemical markers in primary hepatic carcinoma, addresses the challenges faced in this field of study, and anticipates its future application prospects.

1. Introduction

Primary hepatic carcinoma, encompassing hepatocellular carcinoma (HCC), intrahepatic cholangiocarcinoma (ICC), and other rare types, is recognized as the sixth most prevalent tumor globally and the third leading cause of cancer mortality [1]. In contrast to other cancers such as breast, colorectal, and lung cancers, liver cancer presents with notably limited treatment options. These treatments, ranging from surgical interventions to non-surgical approaches like targeted therapies and immune checkpoint inhibitors, often fall short of expected outcomes. Studies suggest that the substantial heterogeneity of primary hepatic carcinoma is a primary factor in its continued elusiveness [2]. This heterogeneity is primarily manifested through the development of cell clusters within the tumor,

* Corresponding author.
** Corresponding author.
E-mail addresses: yinyunqing.jnu@gmail.com (Y. Yin), zhwdetom@163.com (W. Zhang), chen154033@gmail.com (Y. Chen), szjieru0755@126.com (Y. Zhang), shenxinying0755@126.com (X. Shen).
[1] These authors contributed equally to this work.

https://doi.org/10.1016/j.heliyon.2024.e40588
Received 21 February 2024; Received in revised form 28 September 2024; Accepted 19 November 2024
Available online 20 November 2024

exhibiting diverse molecular characteristics and functional differences throughout tumor genesis and evolution. Currently, both tumor cells and their tumor microenvironment (TME) are acknowledged for their heterogeneity [3,4]. Recognizing and identifying this heterogeneity in primary hepatic carcinoma, to determine the population best suited for targeted or immunotherapy, is imperative for the execution of personalized, precision treatment approaches.

In 1941, Coons and colleagues pioneered the use of immunofluorescence for detecting cellular antigens in tissue sections, inaugurating a novel perspective in understanding diseases at the tissue and molecular levels [5]. This technique, integrating immunology with histochemistry, enables the detection of proteins altered by genetic amplifications, mutations, deletions, translocations, as well as alterations mediated by bacteria and viruses, thus deducing molecular genetic abnormalities within cells [6]. Consequently, immunohistochemistry has become a pivotal bridge among various disciplines, including molecular pathology, basic and clinical medicine, and surgery, providing essential auxiliary information for the diagnosis and classification of numerous diseases, especially tumors [7]. In primary hepatic carcinoma, immunohistochemical markers are not only crucial for identifying the origin of tumors and assessing cellular differentiation but also for providing potential insights into treatment responses, thus becoming reliable therapeutic targets. These markers hold significant value in guiding clinical treatment and evaluating prognoses [8], representing an indispensable element in both clinical practice and scientific research in the forthcoming era of personalized medicine [9].

Currently, the detection of immunohistochemical markers predominantly relies on invasive procedures such as surgical pathology or tissue biopsy. However, due to the heterogeneity of tumors, analyzing local tissue samples may not represent the overall condition of the tumor, and some patients may have contraindications to surgery or biopsy. Therefore, exploring early, non-invasive methods that can reflect the overall tumor immunohistochemistry is of significant clinical relevance for the personalized treatment and prognostic assessment of primary hepatic carcinoma. In recent years, the role of medical imaging has rapidly evolved from being primarily a diagnostic tool to a bridge linking various medical disciplines, playing a pivotal role in the context of precision medicine [10,11]. Radiomics has emerged in response, forming a novel interdisciplinary research field that integrates medical imaging, computer science, statistics, and artificial intelligence technologies. Extensive studies have shown [12–14] that radiomics, through validated image analysis methods, can predict the biological behavior and biochemical features of diseases across multiple imaging modalities such as ultrasound (US), computed tomography (CT), magnetic resonance imaging (MRI), and positron emission tomography (PET). This methodology is vital for diagnosing and classifying diseases at the tissue and even cellular levels, and further evaluating treatment responses and prognosis, thus significantly contributing to the advancement of precision medicine. The concept of radiomics was first introduced by Dutch scholar Lambin et al., in 2012, primarily focusing on the extraction of a large number of high-throughput features from medical images for deeper analysis of imaging data. The process includes several key steps: image acquisition, segmentation, feature extraction, selection, and model development and evaluation. Together, these steps enable radiomics to effectively quantify the heterogeneity of tumor tissues in medical imaging [15]. The Rad-score, a core concept in radiomics, simplifies the complex, high-dimensional features extracted from images-such as morphology, texture, and intensity-into a quantifiable score using statistical or machine learning methods [16].

In this review, the current research progress in predicting immunohistochemical markers of primary hepatic carcinoma using radiomic methods is showcased. The significance of immunohistochemical markers for the precision treatment of liver cancer patients is elucidated, emphasizing the risks, challenges, and opportunities that radiomics will encounter in the era of personalized precision medicine.

2. HCC

2.1. Ki67

Ki67 is a protein predominantly located in the nucleolar region, exhibiting high expression in most proliferative malignant cells, thereby serving as a common marker for cell proliferation in various malignancies [17]. Several studies have indicated that elevated levels of Ki67 expression may be associated with a higher risk of recurrence and shorter survival rates, making it a significant marker of clinical deterioration and poor prognosis in HCC [18–20]. Although some research suggests that Ki67 can act as an independent prognostic indicator to assist clinicians in evaluating patient outcomes [18], its variations and regulatory mechanisms in HCC remain to be elucidated. The application of radiomics to predict Ki67 expression in hepatocellular carcinoma has garnered considerable interest among researchers; however, the clinical translation of these studies warrants further contemplation.

Multiple studies [21–24] have explored the potential of US-based radiomics in predicting Ki67 expression in HCC. A prospective study by Dong et al. [22] included 101 HCC patients, performing feature selection on Kupffer phase images from Sonazoid contrast-enhanced US and developing a multivariable logistic regression model. The model achieved an area under the curve (AUC) of 0.873 in the training group and 0.768 in the testing group, indicating that the radiomics model based on enhanced US images has potential for predicting Ki67 expression and histological staging in HCC patients. Qian et al. [24] analyzed preoperative grayscale US images from 118 HCC patients, delineating 2 cm regions both inside and surrounding the tumor as regions of interest. They constructed intratumoral, peritumoral, and combined models, finding that the fusion model, which integrated the most effective intratumoral and peritumoral features, exhibited the best predictive performance with an AUC of 0.870, demonstrating that additional information from surrounding tissues aids in better capturing tumor biology and heterogeneity. In CT-based radiomics studies [25–27], Zhao et al. [26] investigated 208 HCC patients from two institutions, employing multiphasic contrast-enhanced CT images along with clinical data to establish three predictive models: a clinical-radiological (CR) model, a rad-score (R) model, and a clinical-radiological-radiomics (CRR) model. The CRR model displayed the highest diagnostic efficacy; however, no significant difference in AUC was found between the CRR and CR models in internal and external validation cohorts, suggesting that additional radiomic features may not be

necessary for predicting Ki67 expression in HCC. Several studies have also focused on MRI radiomics related to Ki67 in hepatocellular carcinoma [28–33]. Hu et al. [32] utilized Magnetic Resonance Elastography (MRE) to measure the added value of viscoelasticity in predicting Ki67 expression and were the first to integrate deep learning methods, developing a Deep Learning Combined with Radiomics (DLCR) model. This study modeled preoperative conventional MRI from 108 HCC patients, incorporating MRE-derived shear wave velocity (c-map) and phase angle (φ-map) images into the DLCR model. The findings revealed that the c-map and φ-map significantly enhanced the performance of the DLCR model, highlighting the importance of MRE-based viscoelasticity in predicting Ki67 in HCC tumors.

Table 1 summarizes the studies in the literature to date that have evaluated the use of radiomics to preoperatively predict HCC Ki67.

2.2. CK19

Cytokeratin 19 (CK19) is a low molecular weight intermediate filament of the cytoskeleton [34] and serves as a marker for early hepatocytes, hepatic progenitor cells, and cholangiocytes. Typically, CK19 is not expressed or is expressed at low levels in normal hepatocytes, while approximately 10–30 % of HCC cases exhibit CK19 positivity [35]. CK19-positive HCC is associated with aggressive behavior and adverse outcomes, including poorer overall survival and early tumor recurrence following liver resection and transplantation [36]. However, there are currently no approved drugs specifically targeting CK19-positive HCC. Recent experiments have indicated that CK19-positive HCC cells exhibit a unique response to regorafenib treatment, suggesting it may become an effective therapeutic option for these patients [37].

Zhang et al. [38] conducted a multicenter study to predict CK19 expression in HCC patients, demonstrating that the trained clinical model performed quite well (AUC = 0.917). The predictive performance of the combined model significantly improved with the addition of US data, achieving an impressive AUC of 0.995. Several MRI-based studies [39–44] have also reported remarkably high predictive performance for CK19. Notably, Wang et al. [44] extracted radiomic features from preoperative multiphase MRI images of 227 patients pathologically confirmed to have HCC, and developed a combined model incorporating alpha-fetoprotein (AFP) levels and tumor edge enhancement characteristics, which yielded a high AUC. This study also observed that CK19-positive HCC patients had higher AFP levels and more pronounced arterial phase enhancement at the tumor margins. Related literature suggests that these findings are associated with the poorer differentiation, rapid progression, and unfavorable prognosis of CK19-positive HCC [45]. Chen et al. [40] utilized enhanced MRI images from 141 HCC patients collected from two institutions, outlining the tumor's 3D image for feature extraction and analysis. The model achieved sensitivity, specificity, and accuracy values of 0.800, 0.766, and 0.775, respectively. The study also recorded patients' recurrence-free survival (RFS) and compared MRI changes before and after recurrence, identifying intratumoral hemorrhage and peritumoral low signals during the hepatobiliary phase as independent risk factors for HCC recurrence. A radiomic nomogram predicting RFS in HCC patients was established, with a C-index of 0.707, which could assist clinicians in implementing appropriate interventions before disease progression.

2.3. PD-1/PD-L1, PD-L2

Programmed cell death protein 1 (PD-1) is a surface receptor predominantly expressed on T cells. Its primary function is to attenuate T cell activity, preventing autoimmune reactions against normal tissues and maintaining immune tolerance by binding to PD-L1 or PD-L2 ligands on the surface of healthy cells. PD-L1 serves as the main ligand for PD-1; when PD-L1 binds to PD-1, it can inhibit T cell activity and reduce the immune attack on cancer cells [46]. This mechanism has prompted several clinical studies, such as the IMbrave150 trial [47], where the combination of atezolizumab and bevacizumab demonstrated encouraging antitumor activity and safety; and the KEYNOTE-240 trial [48], which explored the efficacy of pembrolizumab in patients with advanced hepatocellular carcinoma. Some research indicates that upregulation of PD-L2 may serve as a compensatory mechanism when PD-L1 function is inhibited [49]. The expression of PD-L2 may provide insights beyond PD-L1, suggesting it could be a promising biomarker for anti-PD-1 targeted therapies.

Wang et al. [50] investigated the feasibility of predicting PD-1 expression in HCC patients using preoperative radiofrequency US. By analyzing multifactorial US features from 40 patients, including direct energy attenuation, spectral skewness, and Rician distribution characteristics, they identified radiomic features associated with PD-1, achieving a prediction accuracy of 92.5 % and an AUC of 94.23 %. Although the results are promising, Wang's study is a feasibility study lacking external validation, which raises concerns about the robustness of the model and the generalizability of the conclusions. Yao et al. [51] reported an AUC of 0.97 for US multimodal radiomics in predicting PD-1. Additionally, multiple studies [52–55] have demonstrated the potential of MRI in predicting immune-related proteins (PD-1, PD-L1, and PD-L2) in HCC patients. Tao et al. [52] extracted radiomic features from MRI images of 108 HCC patients to develop an MRI-based predictive model, which yielded an AUC of 0.871 for predicting PD-L2 expression. Hectors et al. [55] not only assessed the association between MRI imaging features and immune analysis and genomic characteristics in HCC patients but also analyzed the relationships between radiomic, histopathological, and genomic features with early recurrence after liver resection. Despite limitations related to small sample sizes and lack of external validation, this groundbreaking study correlates tumor imaging, histopathology, genomics, and early recurrence, providing a multidimensional perspective for targeting therapies in HCC, particularly regarding the role of immune microenvironment modulation in liver cancer treatment, as evidenced by results from trials such as CheckMate 040 [56] and IMbrave150 [47].

Table 1
Radiomics studies of Ki67 in HCC.

Ref.	Country	N	Type	Imaging modality	Marker	Segmentation	ROI/ VOI	Independent predictors along	Main result	Validation
Zhang et al. [21],2024	China (multi center)	Training:177. ValidationI:77. ValidationII:56	HCC	US	Ki67	Manual, Intra-tumoral	ROI	AFP along with multiple other clinical parameters	AUC:0.870 (training), 0.872 (Validation I), 0.856 (Validation II)	Internal + external
Dong et al. [22],2022 (prospective)	China	Training:71. Validation:30	HCC	US	Ki67	Manual, Intra-tumoral	ROI	No	AUC:0.873(training), 0.768(validation)	Internal
Zhang et al. [23],2023	China (multi center)	Training:168. ValidationI:43. ValidationII:33	HCC	US	Ki67	Manual, Intra-tumoral	ROI	AFP along with multiple other clinical parameters	AUC:0.986 (training), 0.871 (Validation I), 0.742 (Validation II)	Internal + external
Qian et al. [24],2023	China	Training:82. Validation:36	HCC	US	Ki67	Manual, Intra-tumoral and peritumoral	ROI	No	AUC:0.870 (0.751–0.989)	Internal
Wu et al. [25],2022	China	Training:120. Validation:52	HCC	CT	Ki67	Manual, Intra-tumoral	VOI	AFP, Edmondson grades	AUC:0.884(training), 0.819(validation)	Internal
Zhao et al. [26],2023	China (two center)	Training:120. ValidationI:51. ValidationII:37	HCC	CT	Ki67	Manual, Intra-tumoral	VOI	AFP, non-rim APHE, PVTT, TTPVI	AUC: 0.903(training), 0.848(validation)	Internal + external
Wu et al. [27],2020	China	74	HCC	CT	Ki67	Manual, Intra-tumoral	ROI	No	Contrast and correlation were considered independent risk factors of Ki67	No
Li et al. [28],2019 (prospective)	China	83	HCC	MRI	Ki67	Manual, Intra-tumoral	ROI	AFP, Edmondson grades	Misclassification rates:9.64%–15.66 %	No
Fan et al. [29],2021	China	Training:103. Validation:48	HCC	MRI	Ki67	Manual, Intra-tumoral	VOI	AFP	AUC:0.922(training), 0.863(validation)	Internal
Yan et al. [30],2023	China	Training:180. Validation:78	HCC	MRI	Ki67	Manual, Intra-tumoral	ROI	AFP, tumor size, growth type, peritumoral enhancement	AUC:0.876(training), 0.809(validation)	Internal
Yan et al. [31],2023	China	Training:77. Validation:33	HCC	MRI	Ki67	Manual, Intra-tumoral	ROI	AFP, age, rad score	AUC:0.901(training), 0.781(validation)	Internal
Hu et al. [32],2022	China	Training:87. ValidationI:21. ValidationII:43	HCC	MRI	Ki67	Manual, Intra-tumoral	ROI	AFP	AUC : 0.90 ± 0.03 (ValidationI), 0.83 ± 0.03(ValidationII)	Internal + external
Ye et al. [33],2019 (prospective)	China	89	HCC	MRI	Ki67	Manual, Intra-tumoral	VOI	AFP, BCLC-stage, capsule integrity, tumor margin, enhancing capsule	AIC : 73.65, C-index:0.936	No

Note: HCC: Hepatocellular carcinoma; US: Ultrasound; CT: Computed tomography; MRI: Magnetic resonance imaging; ROI: Region of interest; VOI: Volume of interest; AFP: Alpha-fetoprotein; PVTT: Portal vein tumor thrombosis; PPTVI: Tumor thrombus portal vein invasion; BCLC-stage: Barcelona clinic liver cancer staging system; AUC: Area under the curve; AIC: Akaike information criterion; C-index: Concordance index.

2.4. GPC-3

The p53 protein is encoded by the TP53 gene, and the Cancer Genome Atlas (TCGA) database indicates that mutations in this tumor suppressor gene are among the most common genetic alterations in various human malignancies, including liver cancer [57]. Chronic inflammation caused by HBV infection leads to genomic instability in hepatocytes, increasing the incidence of TP53 mutations. Common types of TP53 mutations include missense mutations and truncating mutations. Missense mutations can result in abnormal p53 protein function, while truncating mutations typically lead to protein loss, both of which enhance the incidence of HCC [58]. Although research has focused on incorporating mutant p53 as a viable therapeutic target in clinical oncology, the realization of targeted therapies against p53 remains a challenging endeavor [59].

Wu et al. [60] investigated and analyzed portal venous phase images from preoperative enhanced CT scans of 63 HCC patients. They constructed first-order features using histograms and second-order features using gray-level co-occurrence matrices. Additionally, the researchers assessed the degree and intensity of staining in postoperative pathological sections to semi-quantitatively evaluate the immunoreactivity of liver cancer tissues to p53 detection agents. The p53 immunoreactivity was scored on a scale of 0–4, based on the percentage of p53-positive tumor cells relative to the total number of tumor cells in the sections. Analysis revealed that image features such as smoothness, contrast, correlation, homogeneity, and entropy could predict the p53 mutation status, with AUC values ranging from 0.621 to 0.792. Among these, correlation and entropy exhibited the highest AUC values, suggesting they may be critical factors in distinguishing between p53-positive and p53-negative cases.

2.5. P53

Glypican-3 (GPC-3) is a member of the heparan sulfate proteoglycan family and is overexpressed in most cases of HCC, while its expression is minimal or absent in normal liver tissue (including cirrhotic tissue) [61]. It has become one of the most popular targets for HCC therapy in recent years. Antibody-drug conjugates (ADCs) targeting GPC-3 aim to selectively kill GPC-3-positive cancer cells by linking antibodies to cytotoxic drugs, demonstrating promising efficacy in clinical trials [62]. Additionally, GPC-3-specific CAR T-cell therapy, which utilizes genetically engineered T cells to target and attack GPC-3-expressing HCC cells, is currently being evaluated in several clinical trials to further assess its efficacy, optimal treatment regimens, and potential side effects [63].

Currently, studies on radiomic prediction of GPC-3 [41,64–67] primarily focus on using MRI images as the initial data, with AUC values ranging from 0.844 to 0.943, indicating that predicting GPC-3 levels in HCC patients using MRI is feasible and effective. Except for Geng et al. [41], which is based on SWI images from non-enhanced MRI, the remaining studies [64–67] utilize enhanced MRI images. Among these, Han et al. [64] explored the value of multiphase enhanced MRI in identifying GPC-3-positive HCC. The researchers analyzed the three-dimensional imaging features of tumors from preoperative enhanced MRI of 126 HCC patients, establishing an optimal radiomic model using various algorithms, including Minimum Redundancy Maximum Relevance (MRMR) and recursive feature elimination. They then combined this model with AFP to create a fusion model, visualized as a nomogram, which ultimately showed AUC values of 0.844 in the training set and 0.862 in the validation set.

2.6. PI3K

Phosphoinositide 3-kinase (PI3K) is an integral part of the PI3K-AKT-mTOR pathway and is ubiquitously present in human tissues, serving as a critical regulator of various intracellular functions including cell growth, protein synthesis, cell cycle regulation, and cell movement. Based on structure and substrate specificity, PI3Ks are classified into Class I, Class II, and Class III, with Class I PI3Ks being the most frequently implicated in human diseases. Aberrant activation of the PI3K pathway is associated with various diseases, particularly cancer. In many types of tumors, the PI3K pathway promotes cancer cell proliferation and survival due to gene mutations or overactivation [68]. The PI3K signaling pathway is not only a key mechanism in the development and progression of liver cancer but has also become a significant focus in liver cancer research and treatment. Studies [69] have shown that the mechanism of action of Sorafenib, a therapeutic agent used in liver cancer, is closely associated with the PI3K-AKT pathway.

Liao and colleagues [70] developed an imaging-genomic model combining next-generation sequencing with enhanced CT. They conducted genetic sequencing on surgical samples from 86 patients diagnosed with HCC (training group) and 46 patients included in TCGA database (external validation group) to identify mutations in the PI3K gene. Radiologists qualitatively observed and recorded apparent characteristics from their preoperative enhanced CT images during the plain, arterial, and portal venous phases. These characteristics included tumor size, blood supply vessel thrombosis, delayed central enhancement, "capsule" appearance, necrosis or severe ischemia, peritumoral bile duct dilation, and hepatic capsule retraction. Simultaneously, the entire liver, tumor region, and peritumoral areas (including peritumoral 5 mm, 10 mm, and 20 mm) were delineated as the Region of Interest (ROI), from which over 2600 features were extracted. Feature selection was performed using factor analysis, logistic regression analysis, LASSO regression analysis, and random forest analysis, resulting in the construction of 8 radiomics models. After computation, the model based on the 10 mm peritumoral area in arterial phase images demonstrated the best predictive performance, with an AUC of 0.733.

2.7. VEGF

Vascular endothelial growth factor (VEGF) is a signaling protein that promotes angiogenesis and plays a critical role in normal physiological processes such as wound healing and embryonic development. Previous studies [71] have shown that excessive expression of VEGF aids tumors in forming new blood vessels, thereby facilitating their growth and metastasis. In hypervascular

tumors like HCC, inhibiting blood vessel growth is an important strategy in cancer treatment. Transarterial chemoembolization (TACE) essentially serves as a mechanical "anti-angiogenic" therapy. Bevacizumab targets and inhibits VEGF by blocking its binding to receptors, thereby obstructing tumor angiogenesis and reducing the blood supply to the tumor [72]. In the IMbrave150 trial, the combination of bevacizumab and atezolizumab significantly improved patient survival, establishing it as a standard first-line treatment for unresectable hepatocellular carcinoma [47].

Fan et al. [73] conducted a retrospective study involving 202 patients with pathologically confirmed HCC, randomly assigning them to a training set (n = 142) and a testing set (n = 60). MRI enhanced multiphase images were used for radiomic feature extraction, yielding a total of 1906 features. The top 14 key features were selected using the F-test. Ultimately, a fusion model was developed incorporating AFP, edge irregularity, and the neutrophil-to-lymphocyte ratio (NLR). Testing revealed AUC values of 0.936 for the training group and 0.836 for the testing group. These results suggest that radiomic approaches hold promise in assisting clinicians in selecting more suitable immunotherapies for patients, potentially improving treatment efficacy and overall survival rates.

Table 2 summarizes the studies in the literature to date that have evaluated the use of radiomics to preoperatively predict HCC CK19, PD-1/PD-L1, PD-L2, P53, PC-3, PI3K, the phosphorylation of β-arrestin1 and VEGF.

3. ICC

ICC is a malignant tumor originating from the epithelial cells of the intrahepatic bile ducts and is recognized as the second leading cause of primary liver cancer incidence and mortality worldwide, with increasing rates in recent years [74]. Unlike perihilar and extrahepatic cholangiocarcinoma, patients with ICC typically present with few early symptoms, often leading to late-stage or metastatic disease that exceeds surgical resection criteria, resulting in poor prognosis. Only 20%–30 % of patients are suitable for curative resection. For those with locally unresectable or distant metastatic ICC, systemic therapy may slow disease progression. Over the past two decades, the combination of gemcitabine and cisplatin has been considered the most effective first-line therapy. Recently, two large randomized trials evaluated the effects of adding immune checkpoint inhibitors (ICIs) to standard chemotherapy in patients with advanced cholangiocarcinoma [75,76]. Both the TOPAZ-1 and KEYNOTE-966 trials demonstrated slight improvements in overall survival (OS) and progression-free survival (PFS) without increasing toxicity [77]. The following is a review of studies utilizing radiomic approaches to predict immunohistochemical markers in ICC.

Peng et al. [78] extracted 1076 quantitative feature parameters from preoperative grayscale US images of 128 ICC patients to develop a model predicting multiple pathological indicators of ICC. The AUCs for Ki-67 and CK7 in the testing and validation sets were 0.804 and 0.848, and 0.750 and 0.789, respectively. Qian et al. [79] analyzed preoperative enhanced MRI texture images from 178 ICC patients and established a fusion model based on three independent features: HBV status, arterial edge enhancement, and enhancement pattern, demonstrating excellent predictive performance for Ki-67 expression. Zhang's research team [80] utilized MRI combined with deep learning to predict PD-1/PD-L1 expression in ICC patients. By tracking overall survival (OS), the researchers found that PD-1/PD-L1 positive patients had worse prognoses compared to negative patients. They developed an OS prediction model combining imaging, clinical factors, and pathology, which stratified ICC patients into high-risk and low-risk groups, predicting 1-year, 3-year, and 5-year survival rates. In another study based on enhanced MRI, Zhang et al. [81] categorized 78 ICC patients into inflammatory and non-inflammatory immune phenotypes based on $CD8^+$ T cell density. They analyzed their multiphase enhanced MRI images and recorded OS, finding that a predictive model based on three wavelet features and one 3D feature exhibited the best performance with an AUC of 0.919. Additionally, the researchers noted that inflammatory immune phenotypes had better prognoses than non-inflammatory phenotypes. Studies [82] have indicated that ICIs can relieve suppression on $CD8^+$ T cells, enhancing their ability to attack tumors; generally, a higher quantity of $CD8^+$ T cells in the tumor microenvironment correlates with improved outcomes of immune checkpoint blockade therapy, thereby enhancing patient survival.

4. cHCC-CCA

Combined hepatocellular cholangiocarcinoma (cHCC-CCA) is a rare tumor that exhibits both hepatocellular and biliary differentiation, accounting for less than 5 % of all primary liver cancers, making it significantly less common than HCC and ICC [83,84]. Since the first case of cHCC-CCA was reported in 1903, the definition of this entity and its related terminology have continually evolved. The 2019 WHO classification of digestive system tumors emphasized that the diagnosis of cHCC-CCA should primarily rely on morphological assessment using routine staining, supplemented by additional immunohistochemical staining to refine subtype identification. Despite the increasing clarity in the definition of mixed hepatocellular cholangiocarcinoma and its distinction from other entities, its rarity, complex histological characteristics, and high intra-tumoral heterogeneity continue to pose diagnostic challenges for radiologists and pathologists. Vascular invasion and lymph node metastasis are more common in cHCC-CCA compared to HCC, and its overall prognosis is generally poorer, resembling that of ICC [85].

Currently, research on radiomics in cHCC-CCA is still in relatively early stages; however, some preliminary studies have attempted to enhance the diagnosis, classification, and prognostic assessment of this rare tumor through radiomic analysis. In a study utilizing enhanced MRI to preoperatively predict the cholangiocyte phenotype of hepatocellular carcinoma and assess postoperative prognosis, Chen et al. [86] aimed to predict the co-expression of CK19 and Glypican-3 in liver tumors. The researchers conducted rigorous pathological evaluations and immunohistochemical staining on patients pathologically confirmed to have solitary HCC, defining tumors with concurrent HepPar-1, GPC-3, or GS positivity alongside CK7 and/or CK19 positivity (≥15 %) as cholangiocyte phenotype HCC. They analyzed the enhanced MR images of all cases and established a logistic regression model to predict cholangiocyte phenotype HCC, achieving area under the curve (AUC) values of 0.76 in the training set and 0.73 in the independent validation set.

Table 2
Radiomics studies of CK19、PD-1/PD-L1、PD-L2、P53、GPC-3、PI3K、the phosphorylation of β-arrestin1 and VEGF in HCC.

Ref.	Country	N	Type	Imaging modality	Marker	Segmentation	ROI/ VOI	Independent predictors along	Main result	Validation
Zhang et al. [38], 2022	China (three center)	Training:143. ValidationI:36. ValidationII:35.	HCC	US	CK19	Manual, Intra-tumoral	ROI	AFP along with multiple other clinical parameters	AUC: 0.995(training), 0.867(validation I), 0.862(validation II)	Internal + external
Zhang et al. [39], 2023	China (two center)	Training:168. ValidationI:72. ValidationII:71	HCC	MRI	CK19	Manual, Intra-tumoral	VOI	Radiomics score, AFP, gender, arterial rim enhancement	AUC:0.914(training), 0.855(validation I), 0.795(validation II)	Internal + external
Chen et al. [40], 2021	China (two center)	Training:102. ValidationI:19. ValidationII:20	HCC	MRI	CK19	Manual, Intra-tumoral	VOI	AFP	AUC:0.833(training), 0.614(validation I) , 0.750(validation II)	Internal + external
Geng et al. [41], 2021	China	53	HCC	MRI	CK19	Manual, Intra-tumoral	ROI	No	AUC:0.905	No
Yang et al. [42], 2021	China (multi center)	Training:143. ValidationI:75. ValidationII:39.	HCC	MRI	CK19	Manual, Intra-tumoral	VOI	No	AUC:0.857(training), 0.726(validation I), 0.790(validation II)	Internal + external
Wang et al. [43], 2020	China	Training:159. Validation:68	HCC	MRI	CK19	Unknow, Intra-tumoral	VOI	AFP, arterial rim enhancement pattern, irregular tumor margin, fusion radiomics signature	AUC:0.951(training), 0.822(validation)	Internal
Wang et al. [44], 2019	China	86	HCC	MRI	CK19	Manual, Intra-tumoral	ROI	AFP, arterial rim enhancement, StdSeparation3D texture character	AUC:0.844	No
Wang et al. [50], 2022	China	40	HCC	US	PD-1	Manual, Intra-tumoral	ROI	No	AUC:0.9423	No
Yao et al. [51],2018 (prospective)	China	47	HCC	US	PD-1	Manual, Intra-tumoral	ROI	No	AUC:0.97	No
Tao et al. [52],2023	China	108	HCC	MRI	PD-L2	Manual, Intra-tumoral	VOI	No	AUC:0.955(training), 0.871(validation)	Internal
Gong et al. [54], 2023	China	Training:74. Validation:34	HCC	MRI	PD-1/ PD-L1	Manual, Intra-tumoral	VOI	The presence of satellite nodules	AUC: PD-1:0.946(training), 0.815(validation); PD-L1:0.898(training), 0.779(validation)	Internal
Tian et al. [53],2021	China	Training:83. Validation:20	HCC	MRI	PD-L1	Manual, Intra-tumoral	VOI	No	AUC: 0.897 ± 0.084	Internal
Hectors et al. [55], 2020	America	48	HCC	MRI	PD-L1	Manual, Intra-tumoral	ROI	No	R: 0.41–0.47 , $P < 0.029$	No
Geng et al. [41], 2021	China	53	HCC	MRI	GPC-3	Manual, Intra-tumoral	ROI	No	AUC:0.905	No
Han et al. [64],2023	China	Training:88. Validation:38	HCC	MRI	GPC-3	Manual, Intra-tumoral	VOI	AFP	AUC:0.844(training), 0.862(validation)	Internal
Zhang et al. [65], 2023	China	Training:137. Validation:49	HCC	MRI	GPC-3	Manual, Intra-tumoral	VOI	Radiomics score, age, AFP, non-smooth tumor margin	AUC:0.888(training), 0.800(validation)	Internal
Chong et al. [66], 2023	China	Training:207. Validation:52	HCC	MRI	GPC-3	Manual, Intra-tumoral	VOI	AFP, homogenous T2 signal, hypointensity on hepatobiliary phase	AUC:0.931(training), 0.943(validation)	Internal
Gu et al. [67],2020	China	Training:195. Validation:98	HCC	MRI	GPC-3	Manual, Intra-tumoral	VOI	AFP	AUC:0.926(training), 0.914(validation)	Internal
Wu et al. [60],2019	China	63	HCC	CT	P53	Unknow, Intra-tumoral	ROI	No	ASM, contrast, correlation, IDM, and entropy were	No

(*continued on next page*)

Table 2 (*continued*)

Ref.	Country	N	Type	Imaging modality	Marker	Segmentation	ROI/ VOI	Independent predictors along	Main result	Validation
Liao et al. [70],2022	China (two center)	Training:86. Validation:46	HCC	CT	PI3K	Manual, Intra-tumoral and peritumoral	VOI	No	predictive of P53 mutation, AUC:0.621–0.792 AUC:0.74(training), 0.73(validation)	external
Fan et al. [73],2020	China	Training:142. Validation:60	HCC	MRI	VEGF	Manual, Intra-tumoral	ROI	AFP, irregular tumor margin	AUC:0.936(training), 0.836(validation)	Internal

Note: HCC: Hepatocellular carcinoma; US: Ultrasound; CT: Computed tomography; MRI: Magnetic resonance imaging; ROI: Region of interest; VOI: Volume of interest; CK19: Cytokeratin 19; PD-1: Programmed cell death protein 1; PD-L1: Programmed death-ligand 1; PD-L2: Programmed death-ligand 2; GPC-3: Glypican-3; P53:Tumor protein 53; PI3K:Phosphatidylinositol-3 kinase; VEGF: Vascular endothelial growth factor; AFP: Alpha-fetoprotein; ALT: Alanine aminotransferase; AUC: Area under the curve; R: Pearson correlation coefficient; P: P-value; ASM: Angular second moment; IDM: Inverse difference moment.

Table 3
Radiomics studies in ICC and cHCC-CCA.

Ref.	Country	N	Type	Imaging modality	Marker	Segmentation	ROI/ VOI	Independent predictors along	Main result	Validation
Peng et al. [78],2020	China	Training:90. Validation:38	ICC	US	Ki67	Manual, Intra-tumoral	ROI	No	AUC:0.804 (training, 0.848 (validation)	Internal
Peng et al. [78],2020	China	Training:89. Validation:39	ICC	US	Ck7	Manual, Intra-tumoral	ROI	No	AUC:0.750 (training), 0.789 (validation)	Internal
Peng et al. [78],2020	China	Training:89. Validation:39	ICC	US	VEGF	Manual, Intra-tumoral	ROI	No	AUC:0.760 (training), 0.864 (validation)	Internal
Qian et al. [79],2023 (retrospective-prospective)	China	Training:124. ValidationI:54. ValidationII:49	ICC	MRI	Ki67	Manual, Intra-tumoral	VOI	HBV, arterial rim enhancement, enhancement pattern	AUC:0.860 (training), 0.843 (validation I), 0.815 (validation II)	Internal
Zhang et al. [81],2021	China	78	ICC	MRI	$CD8^{+}$	Manual, Intra-tumoral	VOI	No	AUC：0.919	No
Zhang et al. [80],2020	China	98	ICC	MRI	PD-1/ PD-L1	Manual, Intra-tumoral	VOI	PD-1: pathology, imaging classification, enhancement, intratumour vascularity; PD-L1: No	AUC:0.897(PD-1), 0.890(PD-L1)	Internal
Chen et al. [86],2023	China	Training:232. Validation:102	cHCC-CCA	MRI	CK19+ GPC-3	Manual, Intra-tumoral	ROI	No	AUC:0.760 (training), 0.730 (validation)	Internal

Note: ICC: Intrahepatic cholangiocarcinoma; cHCC-CCA: Combined hepatocellular cholangiocarcinoma; US: Ultrasound; MRI: Magnetic resonance imaging; CK7: Cytokeratin 7; CK19: Cytokeratin 19; GPC-3: Glypican-3; VEGF: Vascular endothelial growth factor; CD8: Cluster of differentiation 8; PD-1: Programmed cell death protein 1; PD-L1: Programmed death-ligand 1; ROI: Region of interest; VOI: Volume of interest; HBV: Hepatitis B virus; AUC: Area under the curve.

Additionally, regular follow-up of patients with cholangiocyte phenotype HCC post-liver resection revealed lower recurrence-free survival (RFS) and overall survival (OS) rates.

Table 3 summarizes the studies in the literature to date that have evaluated the use of radiomics to preoperatively predict ICC and cHCC-CCA immunohistochemical markers.

4.1. Challenge

Despite current advancements in radiomics for predicting HCC immunohistochemistry markers, indicating significant potential in this field, several challenges impede its development and wider acceptance. Non-standardization in image acquisition, subjectivity in defining regions of interest, and inappropriate use of statistical methods have raised concerns about the reproducibility of radiomic studies. These issues often lead to an increased risk of false-positive outcomes in external validation, making the reproducibility of radiomics a major bottleneck in its progression [87]. Furthermore, prominent biomarkers discussed in the review, such as Ki67 and VEGF, are not routinely used in the pathological assessment of primary liver cancer, and their clinical validity remains to be established. The evaluation of these biomarkers is primarily conducted by pathologists, whereas radiomics studies are predominantly led by radiologists, who may overlook crucial issues affecting results, such as the reproducibility of immunostaining and the threshold values for different biomarkers. The majority of these studies are retrospective and single-centered, necessitating further validation through multicentric, large-scale, and prospective trials. Lastly, for clinical application of radiomics in predicting HCC immunohistochemical markers, there is a pressing need for standardized management of large-scale imaging data and the development of specialized software to support these endeavors.

4.2. Outlook

Both radiology and immunohistochemistry technologies utilize visual analysis to generate auxiliary information guiding patient diagnosis. Combining these two approaches in disease diagnosis can enhance diagnostic accuracy and enable more refined subclassification of diseases. Additionally, leveraging radiology to infer immunohistochemical characteristics optimizes the use of imaging resources. This not only reduces unnecessary repeat examinations but also facilitates telemedicine and resource sharing. Furthermore, immunohistochemistry helps in identifying conditions on the tumor cell surface or within the tumor microenvironment, often serving as a basis for subsequent immunotherapy. The radiomics approach undoubtedly accelerates the application of immunohistochemistry in selecting immunotherapy regimens for patients with primary hepatic carcinoma. Personalized treatment based on predicted immunohistochemical outcomes may improve patient prognosis and extend survival, significantly contributing to the advancement of precision medicine.

5. Conclusion

Radiomics has achieved certain milestones in predicting immunohistochemical markers of primary hepatic carcinoma, yet it still confronts numerous challenges, such as reproducibility in radiomic analysis. Unquestionably, the application of radiomics in forecasting immunohistochemical markers for primary hepatic carcinoma not only provides robust support for personalized treatment options for patients but also inevitably propels the advancement of precision medicine.

CRediT authorship contribution statement

Yunqing Yin: Writing – original draft, Visualization, Validation, Investigation, Data curation. **Wei Zhang:** Supervision, Formal analysis, Conceptualization. **Yanhui Chen:** Investigation, Data curation. **Yanfang Zhang:** Writing – review & editing, Validation, Supervision. **Xinying Shen:** Writing – review & editing, Supervision, Data curation.

Ethics approval and consent to participate

Not applicable.

Financial support

No.

Declaration of competing interest

The authors declare that they have no known competing financial interests or personal relationships that could have appeared to influence the work reported in this paper.

Acknowledgments

This project was supported by Shenzhen Science and Technology Program (JCYJ20210324112611031) and Key Technologies for

Precision Surgical Planning and Real-Time Guidance Software in Human-Computer Interaction (2020B010165004).

References

[1] R.L. Siegel, A.N. Giaquinto, A. Jemal, Cancer statistics, 2024, CA A Cancer J. Clin. 74 (1) (2024) 12–49.
[2] N. McGranahan, C. Swanton, Clonal heterogeneity and tumor evolution: past, present, and the future, Cell 168 (4) (2017) 613–628.
[3] D.-C. Lin, A. Mayakonda, H.Q. Dinh, P. Huang, L. Lin, X. Liu, L.-W. Ding, J. Wang, B.P. Berman, E.-W. Song, et al., Genomic and epigenomic heterogeneity of hepatocellular carcinoma, Cancer Res. 77 (9) (2017) 2255–2265.
[4] I. Dagogo-Jack, A.T. Shaw, Tumour heterogeneity and resistance to cancer therapies, Nat. Rev. Clin. Oncol. 15 (2) (2018) 81–94.
[5] A.H. Coons, H.J. Creech, R.N. Jones, Immunological properties of an antibody containing a fluorescent group, Exp. Biol. Med. 47 (2) (1941) 200–202.
[6] P.E. Swanson, Foundations of immunohistochemistry. A practical review, Am. J. Clin. Pathol. 90 (3) (1988) 333–339.
[7] J. Teruya-Feldstein, The immunohistochemistry laboratory: looking at molecules and preparing for tomorrow, Arch. Pathol. Lab Med. 134 (11) (2010) 1659–1665.
[8] Z.E. Chen, F. Lin, Application of immunohistochemistry in gastrointestinal and liver neoplasms: new markers and evolving practice, Arch. Pathol. Lab Med. 139 (1) (2015) 14–23.
[9] S. Magaki, S.A. Hojat, B. Wei, A. So, W.H. Yong, An introduction to the performance of immunohistochemistry, Methods Mol. Biol. 1897 (2019) 289–298.
[10] P. Lambin, R.T.H. Leijenaar, T.M. Deist, J. Peerlings, E.E.C. de Jong, J. van Timmeren, S. Sanduleanu, R.T.H.M. Larue, A.J.G. Even, A. Jochems, et al., Radiomics: the bridge between medical imaging and personalized medicine, Nat. Rev. Clin. Oncol. 14 (12) (2017) 749–762.
[11] L. Hood, S.H. Friend, Predictive, personalized, preventive, participatory (P4) cancer medicine, Nat. Rev. Clin. Oncol. 8 (3) (2011) 184–187.
[12] H. Li, Y. Zhu, E.S. Burnside, E. Huang, K. Drukker, K.A. Hoadley, C. Fan, S.D. Conzen, M. Zuley, J.M. Net, et al., Quantitative MRI radiomics in the prediction of molecular classifications of breast cancer subtypes in the TCGA/TCIA data set, NPJ Breast Cancer 2 (2016), 16012-16012.
[13] T.P. Coroller, P. Grossmann, Y. Hou, E. Rios Velazquez, R.T.H. Leijenaar, G. Hermann, P. Lambin, B. Haibe-Kains, R.H. Mak, H.J.W.L. Aerts, CT-based radiomic signature predicts distant metastasis in lung adenocarcinoma, Radiother. Oncol. 114 (3) (2015) 345–350.
[14] J. Miranda, N. Horvat, G.M. Fonseca, JdAB. Araujo-Filho, M.C. Fernandes, C. Charbel, J. Chakraborty, F.F. Coelho, C.H. Nomura, P. Herman, Current status and future perspectives of radiomics in hepatocellular carcinoma, World J. Gastroenterol. 29 (1) (2023) 43–60.
[15] V. Kumar, Y. Gu, S. Basu, A. Berglund, S.A. Eschrich, M.B. Schabath, K. Forster, H.J.W.L. Aerts, A. Dekker, D. Fenstermacher, et al., Radiomics: the process and the challenges, Magn. Reson. Imaging 30 (9) (2012) 1234–1248.
[16] I. Isupov, M.D.F. McInnes, S.J. Hamstra, G. Doherty, A. Gupta, S. Peddle, Z. Jibri, K. Rakhra, R.M. Hibbert, Development of RAD-score: a tool to assess the procedural competence of diagnostic radiology residents, AJR Am. J. Roentgenol. 208 (4) (2017) 820–826.
[17] L.T. Li, G. Jiang, Q. Chen, J.N. Zheng, Ki67 is a promising molecular target in the diagnosis of cancer, Mol. Med. Rep. 11 (3) (2015) 1566–1572 (review).
[18] W. Shi, J. Hu, S. Zhu, X. Shen, X. Zhang, C. Yang, H. Gao, H. Zhang, Expression of MTA2 and Ki-67 in hepatocellular carcinoma and their correlation with prognosis, Int. J. Clin. Exp. Pathol. 8 (10) (2015) 13083–13089.
[19] J. Cui, B.-W. Dong, P. Liang, X.-L. Yu, D.-J. Yu, Effect of c-myc, Ki-67, MMP-2 and VEGF expression on prognosis of hepatocellular carcinoma patients undergoing tumor resection, World J. Gastroenterol. 10 (10) (2004) 1533–1536.
[20] A. Schmitt-Gräff, V. Ertelt, H.-P. Allgaier, K. Koelble, M. Olschewski, R. Nitschke, M.-L. Bochaton-Piallat, G. Gabbiani, H.E. Blum, Cellular retinol-binding protein-1 in hepatocellular carcinoma correlates with beta-catenin, Ki-67 index, and patient survival, Hepatology 38 (2) (2003) 470–480.
[21] D. Zhang, X.-Y. Zhang, W.-W. Lu, J.-T. Liao, C.-X. Zhang, Q. Tang, X.-W. Cui, Predicting Ki-67 expression in hepatocellular carcinoma: nomogram based on clinical factors and contrast-enhanced ultrasound radiomics signatures, Abdom Radiol (NY) 49 (5) (2024) 1419–1431.
[22] Y. Dong, D. Zuo, Y.-J. Qiu, J.-Y. Cao, H.-Z. Wang, W.-P. Wang, Prediction of histological grades and ki-67 expression of hepatocellular carcinoma based on sonazoid contrast enhanced ultrasound radiomics signatures, Diagnostics 12 (9) (2022).
[23] L. Zhang, S. Duan, Q. Qi, Q. Li, S. Ren, S. Liu, B. Mao, Y. Zhang, S. Wang, L. Yang, et al., Noninvasive prediction of ki-67 expression in hepatocellular carcinoma using machine learning-based ultrasomics: a multicenter study, J. Ultrasound Med. 42 (5) (2023) 1113–1122.
[24] H. Qian, Z. Shen, D. Zhou, Y. Huang, Intratumoral and peritumoral radiomics model based on abdominal ultrasound for predicting Ki-67 expression in patients with hepatocellular cancer, Front. Oncol. 13 (2023) 1209111.
[25] C. Wu, J. Chen, Y. Fan, M. Zhao, X. He, Y. Wei, W. Ge, Y. Liu, Nomogram based on CT radiomics features combined with clinical factors to predict Ki-67 expression in hepatocellular carcinoma, Front. Oncol. 12 (2022) 943942.
[26] Y.-M. Zhao, S.-S. Xie, J. Wang, Y.-M. Zhang, W.-C. Li, Z.-X. Ye, W. Shen, Added value of CE-CT radiomics to predict high Ki-67 expression in hepatocellular carcinoma, BMC Med. Imag. 23 (1) (2023) 138.
[27] H. Wu, X. Han, Z. Wang, L. Mo, W. Liu, Y. Guo, X. Wei, X. Jiang, Prediction of the Ki-67 marker index in hepatocellular carcinoma based on CT radiomics features, Phys. Med. Biol. 65 (23) (2020) 235048.
[28] Y. Li, C. Yan, S. Weng, Z. Shi, H. Sun, J. Chen, X. Xu, R. Ye, J. Hong, Texture analysis of multi-phase MRI images to detect expression of Ki67 in hepatocellular carcinoma, Clin. Radiol. 74 (10) (2019) 813.e819–813.e827.
[29] Y. Fan, Y. Yu, X. Wang, M. Hu, C. Hu, Radiomic analysis of Gd-EOB-DTPA-enhanced MRI predicts Ki-67 expression in hepatocellular carcinoma, BMC Med. Imag. 21 (1) (2021) 100.
[30] Y. Yan, X.S. Lin, W.Z. Ming, Z.Q. Chuan, G. Hui, S.Y. Juan, W. Shuang, L.V. Yang Fan, Z. Dong, Radiomic analysis based on Gd-EOB-DTPA enhanced MRI for the preoperative prediction of Ki-67 expression in hepatocellular carcinoma, Acad. Radiol. 31 (3) (2024) 859–869.
[31] C. Yan, Z. Han, X. Chen, L. Gao, R. Ye, Y. Li, Diffusion-weighted imaging as a quantitative imaging biomarker for predicting proliferation rate in hepatocellular carcinoma: developing a radiomics nomogram, J. Comput. Assist. Tomogr. 47 (4) (2023) 539–547.
[32] X. Hu, J. Zhou, Y. Li, Y. Wang, J. Guo, I. Sack, W. Chen, F. Yan, R. Li, C. Wang, Added value of viscoelasticity for MRI-based prediction of Ki-67 expression of hepatocellular carcinoma using a deep learning combined radiomics (DLCR) model, Cancers 14 (11) (2022).
[33] Z. Ye, H. Jiang, J. Chen, X. Liu, Y. Wei, C. Xia, T. Duan, L. Cao, Z. Zhang, B. Song, Texture analysis on gadoxetic acid enhanced-MRI for predicting Ki-67 status in hepatocellular carcinoma: a prospective study, Chin. J. Cancer Res. 31 (5) (2019) 806–817.
[34] X. Hou, Q. Wu, C. Rajagopalan, C. Zhang, M. Bouhamdan, H. Wei, X. Chen, K. Zaman, C. Li, X. Sun, et al., CK19 stabilizes CFTR at the cell surface by limiting its endocytic pathway degradation, Faseb. J. 33 (11) (2019) 12602–12615.
[35] J.-Y. Zhuo, D. Lu, W.-Y. Tan, S.-S. Zheng, Y.-Q. Shen, X. Xu, CK19-positive hepatocellular carcinoma is a characteristic subtype, J. Cancer 11 (17) (2020) 5069–5077.
[36] O. Govaere, M. Komuta, J. Berkers, B. Spee, C. Janssen, F. de Luca, A. Katoonizadeh, J. Wouters, L.C. van Kempen, A. Durnez, et al., Keratin 19: a key role player in the invasion of human hepatocellular carcinomas, Gut 63 (4) (2014) 674–685.
[37] J. Zhuo, D. Lu, Z. Lin, X. Yang, M. Yang, J. Wang, Y. Tao, X. Wen, H. Li, Z. Lian, et al., The distinct responsiveness of cytokeratin 19-positive hepatocellular carcinoma to regorafenib, Cell Death Dis. 12 (12) (2021) 1084.
[38] L. Zhang, Q. Qi, Q. Li, S. Ren, S. Liu, B. Mao, X. Li, Y. Wu, L. Yang, L. Liu, et al., Ultrasomics prediction for cytokeratin 19 expression in hepatocellular carcinoma: a multicenter study, Front. Oncol. 12 (2022) 994456.
[39] L. Zhang, H. Zhou, X. Zhang, Z. Ding, J. Xu, A radiomics nomogram for predicting cytokeratin 19-positive hepatocellular carcinoma: a two-center study, Front. Oncol. 13 (2023) 1174069.
[40] Y. Chen, J. Chen, Y. Zhang, Z. Lin, M. Wang, L. Huang, M. Huang, M. Tang, X. Zhou, Z. Peng, et al., Preoperative prediction of cytokeratin 19 expression for hepatocellular carcinoma with deep learning radiomics based on gadoxetic acid-enhanced magnetic resonance imaging, J. Hepatocell. Carcinoma 8 (2021) 795–808.

[41] Z. Geng, Y. Zhang, S. Wang, H. Li, C. Zhang, S. Yin, C. Xie, Y. Dai, Radiomics analysis of susceptibility weighted imaging for hepatocellular carcinoma: exploring the correlation between histopathology and radiomics features, Magn. Reson. Med. Sci. 20 (3) (2021) 253–263.
[42] F. Yang, Y. Wan, L. Xu, Y. Wu, X. Shen, J. Wang, D. Lu, C. Shao, S. Zheng, T. Niu, et al., MRI-radiomics prediction for cytokeratin 19-positive hepatocellular carcinoma: a multicenter study, Front. Oncol. 11 (2021) 672126.
[43] W. Wang, D. Gu, J. Wei, Y. Ding, L. Yang, K. Zhu, R. Luo, S.-X. Rao, J. Tian, M. Zeng, A radiomics-based biomarker for cytokeratin 19 status of hepatocellular carcinoma with gadoxetic acid-enhanced MRI, Eur. Radiol. 30 (5) (2020) 3004–3014.
[44] H.-Q. Wang, C. Yang, M.-S. Zeng, S.-X. Rao, Y. Ji, X. Weng, J.-Y. Wang, R.-F. Sheng, Magnetic resonance texture analysis for the identification of cytokeratin 19-positive hepatocellular carcinoma, Eur. J. Radiol. 117 (2019) 164–170.
[45] A.S. Kierans, P. Leonardou, P. Hayashi, L.M. Brubaker, M. Elazzazi, F. Shaikh, R.C. Semelka, MRI findings of rapidly progressive hepatocellular carcinoma, Magn. Reson. Imaging 28 (6) (2010) 790–796.
[46] Y. Ishida, Y. Agata, K. Shibahara, T. Honjo, Induced expression of PD-1, a novel member of the immunoglobulin gene superfamily, upon programmed cell death, EMBO J. 11 (11) (1992) 3887–3895.
[47] R.S. Finn, S. Qin, M. Ikeda, P.R. Galle, M. Ducreux, T.-Y. Kim, M. Kudo, V. Breder, P. Merle, A.O. Kaseb, et al., Atezolizumab plus bevacizumab in unresectable hepatocellular carcinoma, N. Engl. J. Med. 382 (20) (2020) 1894–1905.
[48] R.S. Finn, B.-Y. Ryoo, P. Merle, M. Kudo, M. Bouattour, H.Y. Lim, V. Breder, J. Edeline, Y. Chao, S. Ogasawara, et al., Pembrolizumab as second-line therapy in patients with advanced hepatocellular carcinoma in KEYNOTE-240: a randomized, double-blind, phase III trial, J. Clin. Oncol. : Official Journal of the American Society of Clinical Oncology 38 (3) (2020) 193–202.
[49] D. Umezu, N. Okada, Y. Sakoda, K. Adachi, T. Ojima, H. Yamaue, M. Eto, K. Tamada, Inhibitory functions of PD-L1 and PD-L2 in the regulation of anti-tumor immunity in murine tumor microenvironment, Cancer Immunol. Immunother. 68 (2) (2019) 201–211.
[50] Q. Wang, Y. Dong, T. Xiao, S. Zhang, J. Yu, L. Li, Q. Zhang, Y. Wang, Y. Xiao, W. Wang, Prediction of programmed cell death protein 1 in hepatocellular carcinoma patients using radiomics analysis with radiofrequency-based ultrasound multifeature maps, Biomed. Eng. Online 21 (1) (2022) 24.
[51] Z. Yao, Y. Dong, G. Wu, Q. Zhang, D. Yang, J.-H. Yu, W.-P. Wang, Preoperative diagnosis and prediction of hepatocellular carcinoma: radiomics analysis based on multi-modal ultrasound images, BMC Cancer 18 (1) (2018) 1089.
[52] Y.-Y. Tao, Y. Shi, X.-Q. Gong, L. Li, Z.-M. Li, L. Yang, X.-M. Zhang, Radiomic analysis based on magnetic resonance imaging for predicting PD-L2 expression in hepatocellular carcinoma, Cancers 15 (2) (2023).
[53] Y. Tian, T.E. Komolafe, J. Zheng, G. Zhou, T. Chen, B. Zhou, X. Yang, Assessing PD-L1 expression level via preoperative MRI in HCC based on integrating deep learning and radiomics features, Diagnostics 11 (10) (2021).
[54] X.Q. Gong, N. Liu, Y.Y. Tao, L. Li, Z.M. Li, L. Yang, X.M. Zhang, Radiomics models based on multisequence MRI for predicting PD-1/PD-L1 expression in hepatocellular carcinoma, Sci. Rep. 13 (1) (2023) 7710.
[55] S.J. Hectors, S. Lewis, C. Besa, M.J. King, D. Said, J. Putra, S. Ward, T. Higashi, S. Thung, S. Yao, et al., MRI radiomics features predict immuno-oncological characteristics of hepatocellular carcinoma, Eur. Radiol. 30 (7) (2020) 3759–3769.
[56] A.B. El-Khoueiry, B. Sangro, T. Yau, T.S. Crocenzi, M. Kudo, C. Hsu, T.-Y. Kim, S.-P. Choo, J. Trojan, T.H. Welling, et al., Nivolumab in patients with advanced hepatocellular carcinoma (CheckMate 040): an open-label, non-comparative, phase 1/2 dose escalation and expansion trial, Lancet 389 (10088) (2017) 2492–2502.
[57] J.M. Nigro, S.J. Baker, A.C. Preisinger, J.M. Jessup, R. Hostetter, K. Cleary, S.H. Bigner, N. Davidson, S. Baylin, P. Devilee, Mutations in the p53 gene occur in diverse human tumour types, Nature 342 (6250) (1989) 705–708.
[58] A. Villanueva, Y. Hoshida, Depicting the role of TP53 in hepatocellular carcinoma progression, J. Hepatol. 55 (3) (2011) 724–725.
[59] F. Mantovani, D. Walerych, G.D. Sal, Targeting mutant p53 in cancer: a long road to precision therapy, FEBS J. 284 (6) (2017) 837–850.
[60] H. Wu, X. Chen, J. Chen, Y. Luo, X. Jiang, X. Wei, W. Tang, Y. Liu, Y. Liang, W. Liu, et al., Correlations between P53 mutation status and texture features of CT images for hepatocellular carcinoma, Methods Inf. Med. 58 (1) (2019) 42–49.
[61] M. Guo, H. Zhang, J. Zheng, Y. Liu, Glypican-3: a new target for diagnosis and treatment of hepatocellular carcinoma, J. Cancer 11 (8) (2020) 2008–2021.
[62] Y. Fu, D.J. Urban, R.R. Nani, Y.-F. Zhang, N. Li, H. Fu, H. Shah, A.P. Gorka, R. Guha, L. Chen, et al., Glypican-3-Specific antibody drug conjugates targeting hepatocellular carcinoma, Hepatology 70 (2) (2019) 563–576.
[63] N. Pang, J. Shi, L. Qin, A. Chen, Y. Tang, H. Yang, Y. Huang, Q. Wu, X. Li, B. He, et al., IL-7 and CCL19-secreting CAR-T cell therapy for tumors with positive glypican-3 or mesothelin, J. Hematol. Oncol. 14 (1) (2021) 118.
[64] Z. Han, H. Dai, X. Chen, L. Gao, X. Chen, C. Yan, R. Ye, Y. Li, Delta-radiomics models based on multi-phase contrast-enhanced magnetic resonance imaging can preoperatively predict glypican-3-positive hepatocellular carcinoma, Front. Physiol. 14 (2023) 1138239.
[65] N. Zhang, M. Wu, Y. Zhou, C. Yu, D. Shi, C. Wang, M. Gao, Y. Lv, S. Zhu, Radiomics nomogram for prediction of glypican-3 positive hepatocellular carcinoma based on hepatobiliary phase imaging, Front. Oncol. 13 (2023) 1209814.
[66] H. Chong, Y. Gong, Y. Zhang, Y. Dai, R. Sheng, M. Zeng, Radiomics on gadoxetate disodium-enhanced MRI: non-invasively identifying glypican 3-positive hepatocellular carcinoma and postoperative recurrence, Acad. Radiol. 30 (1) (2023) 49–63.
[67] D. Gu, Y. Xie, J. Wei, W. Li, Z. Ye, Z. Zhu, J. Tian, X. Li, MRI-based radiomics signature: a potential biomarker for identifying glypican 3-positive hepatocellular carcinoma, J. Magn. Reson. Imag. 52 (6) (2020) 1679–1687.
[68] R.R. Madsen, PI3K in stemness regulation: from development to cancer, Biochem. Soc. Trans. 48 (1) (2020) 301–315.
[69] Y. Sun, H. Zhang, J. Meng, F. Guo, D. Ren, H. Wu, X. Jin, S-palmitoylation of PCSK9 induces sorafenib resistance in liver cancer by activating the PI3K/AKT pathway, Cell Rep. 40 (7) (2022) 111194.
[70] H. Liao, H. Jiang, Y. Chen, T. Duan, T. Yang, M. Han, Z. Xue, F. Shi, K. Yuan, M.R. Bashir, et al., Predicting genomic alterations of phosphatidylinositol-3 kinase signaling in hepatocellular carcinoma: a radiogenomics study based on next-generation sequencing and contrast-enhanced CT, Ann. Surg Oncol. 29 (2022) 4552–4564.
[71] R.S. Apte, D.S. Chen, N. Ferrara, VEGF in signaling and disease: beyond discovery and development, Cell 176 (6) (2019) 1248–1264.
[72] R.S. Finn, A.X. Zhu, Targeting angiogenesis in hepatocellular carcinoma: focus on VEGF and bevacizumab, Expet Rev. Anticancer Ther. 9 (4) (2009) 503–509.
[73] T. Fan, S. Li, K. Li, J. Xu, S. Zhao, J. Li, X. Zhou, H. Jiang, A potential prognostic marker for recognizing VEGF-positive hepatocellular carcinoma based on magnetic resonance radiomics signature, Front. Oncol. 12 (2022) 857715.
[74] V. Porreca, C. Barbagallo, E. Corbella, M. Peres, M. Stella, G. Mignogna, B. Maras, M. Ragusa, C. Mancone, Unveil intrahepatic cholangiocarcinoma heterogeneity through the lens of omics and multi-omics approaches, Cancers 16 (16) (2024).
[75] H.A. Burris, T. Okusaka, A. Vogel, M.A. Lee, H. Takahashi, V. Breder, J.-F. Blanc, J. Li, M. Bachini, M. Żotkiewicz, et al., Durvalumab plus gemcitabine and cisplatin in advanced biliary tract cancer (TOPAZ-1): patient-reported outcomes from a randomised, double-blind, placebo-controlled, phase 3 trial, Lancet Oncol. 25 (5) (2024) 626–635.
[76] R.K. Kelley, M. Ueno, C. Yoo, R.S. Finn, J. Furuse, Z. Ren, T. Yau, H.-J. Klümpen, S.L. Chan, M. Ozaka, et al., Pembrolizumab in combination with gemcitabine and cisplatin compared with gemcitabine and cisplatin alone for patients with advanced biliary tract cancer (KEYNOTE-966): a randomised, double-blind, placebo-controlled, phase 3 trial, Lancet 401 (10391) (2023) 1853–1865.
[77] K. Almhanna, Immune checkpoint inhibitors in combination with chemotherapy for patients with biliary tract cancer: what did we learn from TOPAZ-1 and KEYNOTE-966, Transl. Cancer Res. 13 (1) (2024) 22–24.
[78] Y.-T. Peng, C.-Y. Zhou, P. Lin, D.-Y. Wen, X.-D. Wang, X.-Z. Zhong, D.-H. Pan, Q. Que, X. Li, L. Chen, et al., Preoperative ultrasound radiomics signatures for noninvasive evaluation of biological characteristics of intrahepatic cholangiocarcinoma, Acad. Radiol. 27 (6) (2020) 785–797.
[79] X. Qian, C. Zhou, F. Wang, X. Lu, Y. Zhang, L. Chen, M. Zeng, Development and validation of combined Ki67 status prediction model for intrahepatic cholangiocarcinoma based on clinicoradiological features and MRI radiomics, Radiol. Med. 128 (3) (2023) 274–288.
[80] J. Zhang, Z. Wu, X. Zhang, S. Liu, J. Zhao, F. Yuan, Y. Shi, B. Song, Machine learning: an approach to preoperatively predict PD-1/PD-L1 expression and outcome in intrahepatic cholangiocarcinoma using MRI biomarkers, ESMO Open 5 (6) (2020) e000910.

[81] J. Zhang, Z. Wu, J. Zhao, S. Liu, X. Zhang, F. Yuan, Y. Shi, B. Song, Intrahepatic cholangiocarcinoma: MRI texture signature as predictive biomarkers of immunophenotyping and survival, Eur. Radiol. 31 (6) (2021) 3661–3672.
[82] D.S. Chen, I. Mellman, Elements of cancer immunity and the cancer-immune set point, Nature 541 (7637) (2017) 321–330.
[83] E. Brunt, S. Aishima, P.-A. Clavien, K. Fowler, Z. Goodman, G. Gores, A. Gouw, A. Kagen, D. Klimstra, M. Komuta, et al., cHCC-CCA: consensus terminology for primary liver carcinomas with both hepatocytic and cholangiocytic differentation, Hepatology 68 (1) (2018) 113–126.
[84] A. Beaufrère, J. Calderaro, V. Paradis, Combined hepatocellular-cholangiocarcinoma: an update, J. Hepatol. 74 (5) (2021) 1212–1224.
[85] K. Wakizaka, H. Yokoo, T. Kamiyama, M. Ohira, K. Kato, Y. Fujii, K. Sugiyama, N. Okada, T. Ohata, A. Nagatsu, et al., Clinical and pathological features of combined hepatocellular-cholangiocarcinoma compared with other liver cancers, J. Gastroenterol. Hepatol. 34 (6) (2019) 1074–1080.
[86] Y. Chen, J. Chen, C. Yang, Y. Wu, H. Wei, T. Duan, Z. Zhang, L. Long, H. Jiang, B. Song, Preoperative prediction of cholangiocyte phenotype hepatocellular carcinoma on contrast-enhanced MRI and the prognostic implication after hepatectomy, Insights Into Imaging 14 (1) (2023) 190.
[87] J.E. van Timmeren, D. Cester, S. Tanadini-Lang, H. Alkadhi, B. Baessler, Radiomics in medical imaging-"how-to" guide and critical reflection, Insights Into Imaging 11 (1) (2020) 91.